

Deformable mirror based on piezoelectric actuators for the adaptive system of the Iskra-6 facility

S.Yu. Bokalo, S.G. Garanin, S.V. Grigorovich, V.G. Zhupanov, M.O. Kolygin, S.M. Kulikov, D.M. Lyakhov, A.N. Manachinskii, P.P. Mizin, A.V. Ogorodnikov, V.P. Smekalin, S.P. Smyshlyaev, S.A. Sukharev, O.I. Shanin, V.I. Shchipalkin

Abstract. The main problem in developing high-power pulsed laser facilities (NIF, LMJ, and Iskra-6) is to provide the required quality of their output radiation. For this purpose, adaptive optical systems (AOSs) are used in all these facilities. The present research is devoted to determining the characteristics and working out the most troublesome elements of the AOS – the wavefront sensor and wide-aperture adaptive mirror for the Iskra-6 facility.

Keywords: Nd:glass laser, adaptive optical system, wavefront sensor, adaptive mirror.

1. Introduction

All new generation high-power laser systems developed by National Ignition Facility (NIF, USA) [1], Laser Megajoule (LMJ, France) [2] and Iskra-6 (Russia) [3] emit 3–5-ns pulses at 1.053 μm with the output energy up to 2 MJ (for NIF and LMJ) and 300 kJ (Iskra-6). The ‘Luch’ facility, a module of the Iskra-6 facility, is currently in operation [4, 5]. The most important problem after the attainment of the required output power is to produce radiation with the desired quality. For this purpose, adaptive optical systems (AOSs) are envisaged in all three devices [6, 7] for correcting the aberrations in the ‘cold’ optical path (the so-called static aberrations) and phase distortions caused by the heating of active elements by pump radiation (‘thermal’ aberrations). The static aberrations can be corrected in a closed AOS before operation of the system, and no stringent requirements are imposed on the pulse repetition rate of the system (1–10 Hz). ‘Thermal’ aberrations are corrected by presetting the shape of the optical surface of the deformable mirror from the results of the previous investigations of the wavefronts, i.e., the mirror is subjected

to programmed control. Thus, two types of control loops can be realised in the system – a direct control of the deformable mirror from wavefront measurements and feedback control. The need for measurement of the wavefront shape almost inevitably requires the use of an operating system for phase conjugation [8]. The main elements of such a system are a wavefront sensor (WFS), a deformable mirror (DM), a computer with control software, and amplifying instruments. In the present study, the amplifying instruments and the response speed of the control software are not vital, and hence this research is mainly devoted to the working out of the most vulnerable elements of the AOS – the wavefront sensor and wide-aperture adaptive mirror, and to the evaluation of their parameters.

2. Position of the WFS and DM in the optical scheme of the facility

Figure 1 shows a version of the optical scheme of one of the channels of the Iskra-6 facility [3]. After emerging from the beam forming system (BFS), laser radiation is reflected from small DM (13), enters the spatial transport filter, is reflected from wide-aperture DM (12) after the first pass, is directed to Pockels cell (2) through lens (5) with the help of a deflecting mirror after the second pass, is again reflected from wide-aperture DM (12) after the third pass, and is directed to the target after the fourth pass.

The requirements imposed on WFS are quite different for direct control of the deformable mirror from the measured wavefront and feedback control. In the former case, the WFS must have a wide dynamic range, while in the latter case it only produces the error signal (zero signal in the ideal case) and the dynamic range demands are much lower in this case. However, constraints are imposed as regards linearity, precision and time constant for a stable operation of the control loop. The last requirement is much milder because the control loop may be quite sluggish. Hence, it is expedient to use one WFS with a wide dynamic range in the scheme for measuring the total aberration of the wavefront of radiation after its emergence from the channel. But the deformable mirror can be placed at different positions on the optical path from the place where it leaves the system of its formation to the position where the radiation emerges from the channel. A system with two mirrors placed at different positions on the optical path (see Fig. 1) can also be used.

From the point of view of the requirements imposed on the mirror and the control system, positioning of the mirror

S.Yu. Bokalo, V.G. Zhupanov, D.M. Lyakhov, P.P. Mizin, V.P. Smekalin, O.I. Shanin, V.I. Shchipalkin Federal State Unitary Enterprise, ‘Luch’ Research Institute and Research and Production Association, ul. Zheleznodorozhnaya 24, 142100 Podolsk, Moscow region, Russia; e-mail: oshanin@luch.podolsk.ru;
S.G. Garanin, S.V. Grigorovich, M.O. Kolygin, S.M. Kulikov, A.N. Manachinskii, A.V. Ogorodnikov, S.P. Smyshlyaev, S.A. Sukharev Russian Federal Nuclear Centre ‘All-Russian Scientific Research Institute of Experimental Physics’, prosp. Mira 37, 607190 Sarov, Nizhnii Novgorod region, Russia; e-mail: garanin@otd13.vniif.ru

Received 20 February 2007

Kvantovaya Elektronika 37 (8) 691–696 (2007)

Translated by Ram Wadhwa

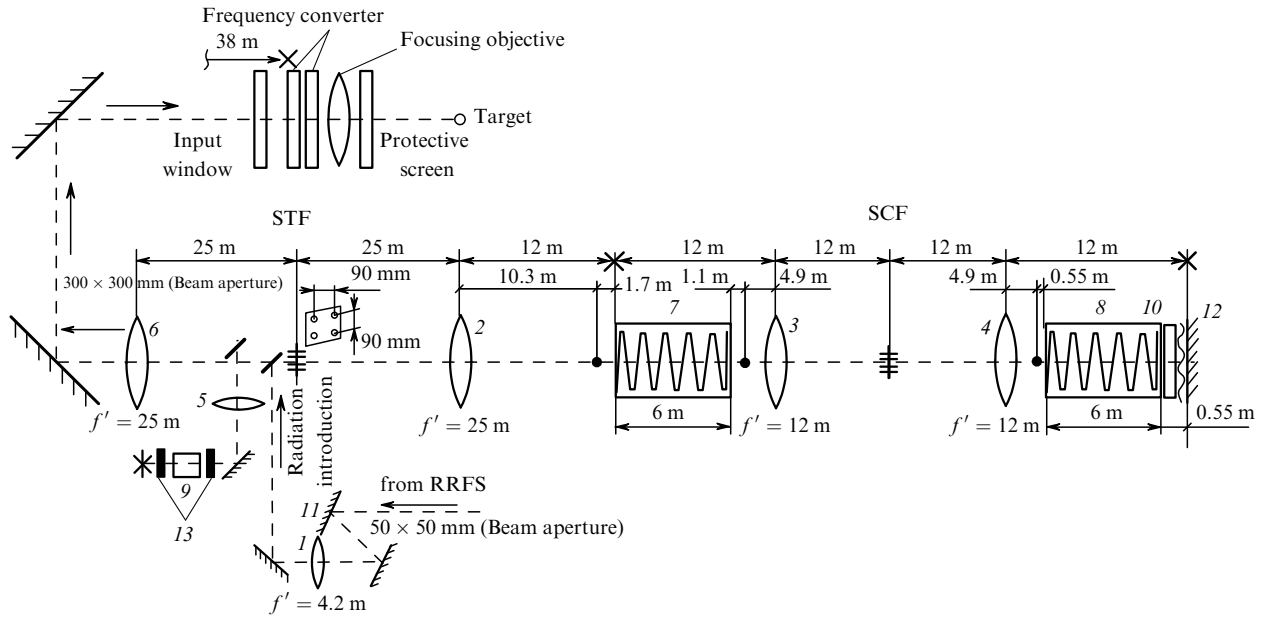


Figure 1. Version of the optical scheme of a channel in the Iskra-6 facility (total length of the channel 110 m): (1)–(6) lenses; (7), (8) mode amplifiers; (9), (10) Pockels cells; (11), (12) deformable mirrors; (13) polarisers; (RRFS) reference radiation formation system; (STF) spatial transport filter; (SCF) spatial cell filter; crosses are used to mark the planes that are conjugate with the deformable mirror, points indicates the positions of focusing of first-order back-reflected signals.

at the beginning or end of the optical path is a limiting case. In the former case, it is difficult to realise a reasonable spatial resolution for an aperture of 50×50 mm (the spacing between the actuators must not exceed 3.5 mm) and the angular selection for the first passes of radiation in the amplifier is hampered. The latter situation requires a high radiation stability of the wide-aperture (300×300 mm) mirror {the assured radiation stability margin should be 1.5–2 times higher than the output energy density (10 J cm^{-2}) [9]} and a large dynamic range. Moreover, the angular selection deteriorates at the last two passes. Installation of two DMs on the path may slightly ease the requirements on each of them, but doubles the number of adaptive optical system elements. If the mirror is positioned behind mode amplifier (8), radiation is reflected twice from it, after the first and third passes. Obviously, this version is most balanced from the point of view of not only angular selection and radiation correction over the entire optical path, but also the requirements imposed on the mirror. In addition, installation of a mirror behind amplifier (8) makes

the requirements on the radiation resistance as well as on the actuator less stringent both as regards its dynamic range and its power characteristics. It also entails a decrease in the capacity and cost of the actuator, power and cost of the control devices, and hence the cost of the system as a whole.

3. Wavefront sensor

It was mentioned above that the ‘Luch’ facility is a prototype of the Iskra-6 facility. A Hartmann type WFS, whose scheme and photograph are shown in Fig. 2, was used for measuring the wavefront of the output laser radiation in the ‘Luch’ facility.

A coupling telescope was used for matching beam aperture with the size of the detection area element of the CCD camera. A variable attenuator ensured the required energy density on this area element. A kinoform consisting of a regular array of Fresnel diffraction lenses (subapertures) in quadratic packing was installed in the plane conjugate to the plane of the deformable mirror and.

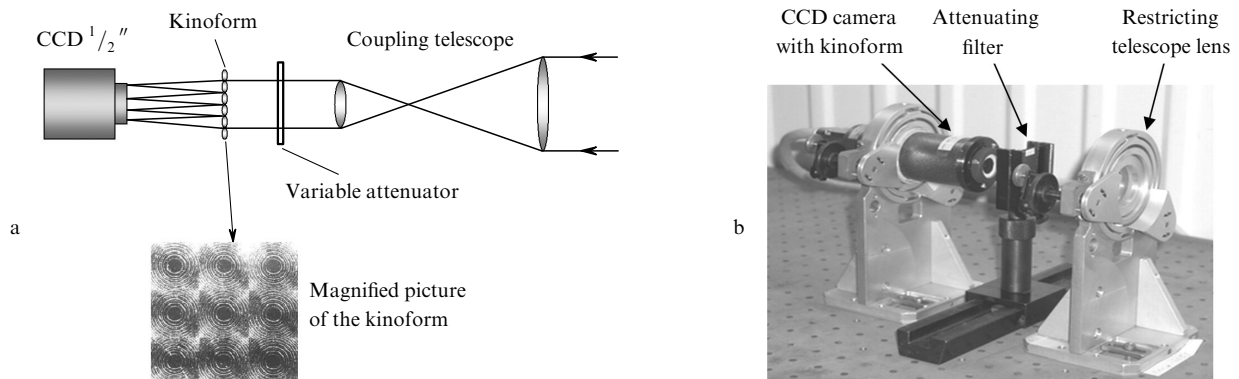


Figure 2. (a) Optical diagram and (b) outward appearance of a WFS.

The rasters were prepared by etching quartz glass substrates using a photomask. The distinguishing features of rasters are a high precision of preparation and identity of individual elements as well as a high diffraction efficiency (85 % of the energy is concentrated in the first diffraction order).

The raster in the WFS serves to form a system of focal spots on the CCD camera whose displacement relative to the centers of the raster subapertures is determined by the local slope of the wavefront. This allows us to reconstruct the wavefront of the radiation incident on the kinoform. The WFS registers the pattern of focal spots of the kinoform whose displacements are used for reconstructing the wavefront surface.

The wavefront surface is reconstructed by measuring the gradients (deviations of focal spots). The reconstruction algorithm is based on reconstruction of the wavefront surface using the Fried discretisation technique [10].

The statistical aberrations of the wavefront were measured at the exit from the optical path of the 'Luch' facility with a resolution of 0.07 points mm⁻¹ (14 × 14 measuring points). Each reconstructed phase point of the wavefront corresponds to a beam region of size 14 × 14 mm, and information about aberration in such regions is lost. Experimental information on wavefronts was used for selecting the parameters of a wide-aperture DM.

4. Determining the number of actuators and their arrangement on the DM aperture

The choice of the number of actuators and their arrangement on the DM aperture to eliminate the aberrations with a given residual error in correction is a problem of fundamental importance. It was shown by using the technique described in [11] that for this purpose at least 121 actuators, i.e., 11 × 11 rows must be available on the aperture for arranging them on a square mesh. In the case of staggered packing, such a number of rows can be realised for 60–61 actuators. Various staggered arrangements of actuators were studied. The correctness of the computational technique is confirmed by experiments with a DM model (see Sec. 5).

4.1 Approximation of aberrations

The experimental data on the wavefront aberrations $W(x, z)$ subjected to correction were approximated by a polynomial consisting of functions describing the intrinsic vibrations of a plate with free edges [12]:

$$W(x, z) = \sum_i \sum_j a_{ij} f(k_i, x) f(k_j, z), \quad (1)$$

where $f(k_i, x)$ and $f(k_j, z)$ are functions describing the intrinsic vibrations of the plate; x and z are normalised coordinates ($0 \leq x \leq 1$, $0 \leq z \leq 1$); k_i and k_j are dimensionless spatial frequencies of intrinsic vibrations,

$$f(k_i, x) = A \left\{ - \left(\frac{-\sin k_i + \sinh k_i}{-\cos k_i + \cosh k_i} \right) \right.$$

$$\left. \times [\cos(k_i x) + \cosh(k_i x)] + [\sin(k_i x) + \sinh(k_i x)] \right\} + a + bx;$$

and A , a and b are certain coefficients. The number of coefficients of the polynomial is often equal to the number of points characterising the measured wavefront. Under

these conditions, the root-mean-square deviation (RMSD) σ of the obtained polynomials from the experimental results was found to be equal to zero for the given set.

4.2 Calculation of the optical surface shape

It was assumed in calculations that the action of actuators is equivalent to the action of forces applied at the given points to a square plate with free edges.

Using the methods of virtual displacements and superposition, we can obtain a relation between the applied forces \mathbf{P} and the coefficients of polynomial (1) which are denoted by their vector $\boldsymbol{\theta}$:

$$\boldsymbol{\theta} = D^{-1} \mathbf{M}^{-1} \mathbf{F} \mathbf{P}, \quad (2)$$

Where D is the cylindrical rigidity of the plate; \mathbf{F} is the matrix of numerical values of the intrinsic vibrations amplitude at the given points; and $2\mathbf{M}/D$ is the diagonal matrix of the energies of intrinsic vibrations.

In view of the orthonormality of the functions describing the intrinsic vibrations, the RMSD of the computed surface from the given surface can be written in the form

$$\sigma = [(\mathbf{B} - \boldsymbol{\theta})^T (\mathbf{B} - \boldsymbol{\theta})]^{1/2}, \quad (3)$$

where \mathbf{B} is the vector of coefficients of polynomial (1) which approximates a certain aberration.

Taking into account formulas (2) and (3), we define the forces ensuring the minimum of $(\mathbf{B} - \boldsymbol{\theta})^T (\mathbf{B} - \boldsymbol{\theta})$, and hence the required form of the mirror surface. These forces are calculated with the help of the formula

$$\mathbf{P}' = (\mathbf{A}^T \mathbf{F}^T \mathbf{M}^{-1} \mathbf{M}^{-1} \mathbf{F} \mathbf{A})^{-1} \mathbf{A}^T \mathbf{F}^T \mathbf{M}^{-1} \mathbf{B} \mathbf{D}, \quad (4)$$

where \mathbf{A} is a matrix that ensures the fulfilment of conditions under which the sums of moments and forces described by the vector \mathbf{P} ($\mathbf{P} = \mathbf{A} \mathbf{P}'$) are equal to zero.

4.3 Analysis of the given experimental wavefronts

Using the technique described above, we calculated the coefficients approximating the polynomials for experimental static and 'thermal' aberrations of the 'Luch' facility. By way of an example, Fig. 3 shows one of the realisations of the measured aberrations and the corresponding spectra of series expansions (1).

An analysis of the available data array reveals that the anisotropy along the spatial frequency axes of the wavefront is clearly visible except in two cases. As a rule, the coefficients a_{ij} remain significant up to the 14th order of expansion. Apparently, it is the wavefront anisotropy that accounts for different numbers of rows (7 and 11) of actuators along the vertical and horizontal directions in the DM installed at the NIF [6].

4.4 Required number of actuators and their arrangement in the aperture

The coefficients obtained as a result of approximation were used to compute the forces required for processing the given geometry of the elastic plate surface. We considered the staggered arrangement of 32 actuators as well as 41 and 61 actuators. For all the versions of the wavefront aberrations, only the DM with 61 actuators was found to be acceptable from the point of view of the admissible error. Figure 4 shows the spectra of coefficients characterising the shape of

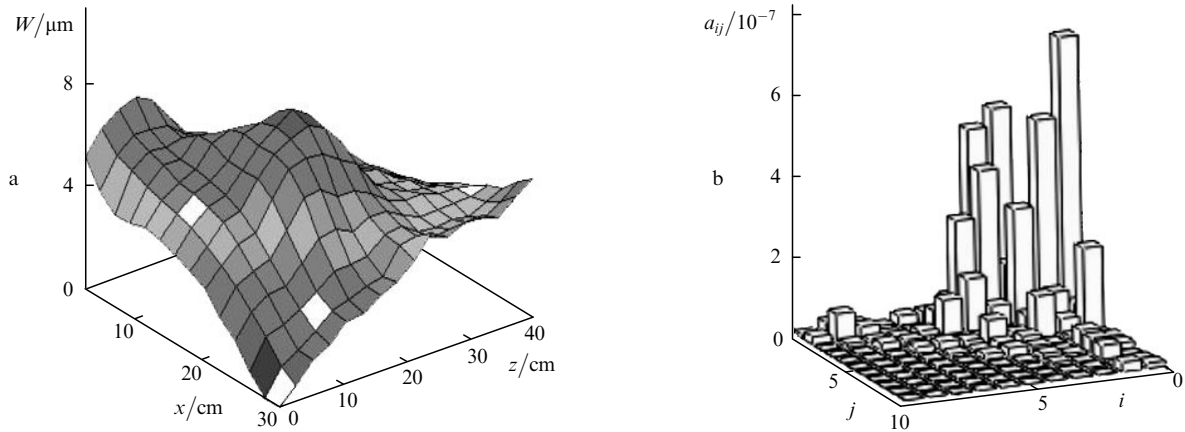


Figure 3. (a) Wavefront shape and (b) spectrum of expansion coefficients for its approximation.

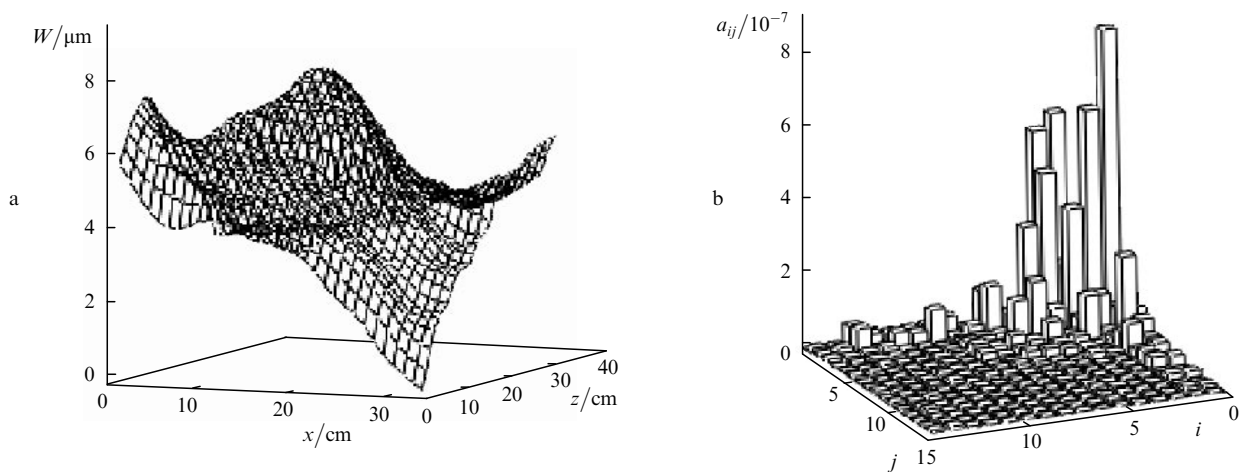


Figure 4. (a) Shape of the surface of a mirror with 61 actuators and (b) spectrum of expansion coefficients for its approximation.

the calculated transverse deviations of the mirror with 61 actuators. The figure also shows the shape of the computed surface. The RMSD between the surfaces shown in Figs 3a and 4a was $0.114 \mu\text{m}$.

Staggered arrangement of actuators in the DM aperture is in good agreement with the squared packing of lenses in the kinoform of the WFS. We should use 12×12 measurement points on the WFS and optically match them with WFS in such a way that four peripheral points of measurements correspond to each actuator. Fried approximation technique also falls in line with this concept. This raises hopes of constructing an effective control algorithm.

5. Model of DM and results of tests

The obtained parameters were used to design, develop and test a nine-channel model of the deformable mirror. Figure 5 shows the outward appearance of the model without protecting cover, casing and knobs.

The mirror plate was made of optical glass ceramic. A coating with a specular reflection coefficient of at least 99.3% was deposited on the polished front optical surface of the plate. The radiation resistance was not less than 20 J cm^{-2} for a radiation pulse duration of 3 ns [13].

Piezoelectric actuators in the form of hollow ceramic cylinders consisting of many layers of the PZT-19 piezo-

ceramic reinforced by a central spindle were used as control actuators. In the free state, such a piezoactuator is displaced by no less than $\pm 24 \mu\text{m}$ under a working voltage of $\pm 300 \text{ V}$. A nosepiece and a stem for subsequent connection of the actuator to the mirror plate and casing were attached to each actuator. All the actuators were arranged in a square mesh.

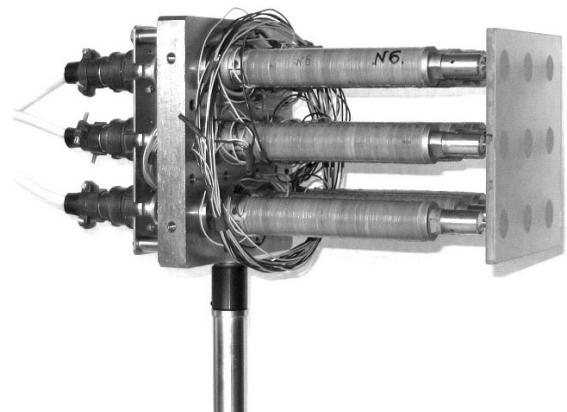


Figure 5. Model of an adaptive mirror.

Table 1. Parameters of actuators at various stages of mirror preparation (working voltage across the actuator was ± 300 V).

Actuator parameters	Actuator No.								
	1	2	3	4	5	6	7	8	9
Static capacitance/ μF	1.043	1.168	1.144	1.091	1.053	1.158	1.066	1.166	1.157
Displacements in initial state/ μm	+27.0	+30.5	+29.2	+30.1	+31.0	+33.5	+28.4	+32.2	+31.2
	-30.0	-30.0	-31.7	-26.5	-26.5	-29.5	-27.0	-28.0	-29.5
Mean displacement/ μm	28.5	30.25	30.45	28.3	28.75	31.5	27.7	30.1	30.35
Displacement for fixture at the plate/ μm	+23.3	+28.0	+25.6	+26.0	+25.0	27.0	+24.3	+26.6	+25.7
	-32.6	-30.5	-33.8	-29.1	-32.0	-36.0	-27.2	-33.8	-33.7
Mean displacement/ μm	27.95	29.25	29.7	27.55	28.5	31.5	25.75	30.2	29.7
Displacement with the mirror/ μm	+24.6	+18.9	+22.7	+18.9	+15.1	+18.9	+20.8	+20.8	+22.7
	-18.9	-17.0	-18.9	-17.0	-13.2	-17.0	-17.0	-17.0	-18.9
Mean displacement/ μm	21.75	17.95	20.8	17.95	14.15	17.95	18.9	18.9	20.8
Average sensitivity/ $\mu\text{m kV}^{-1}$	72.5	59.8	69.3	59.8	47.2	59.8	63	63	69.3
Ratio of the mean displacement with mirror to the initial mean value	0.763	0.593	0.683	0.634	0.492	0.570	0.682	0.628	0.685

The casing was made of invar. The stems of the control actuators were fastened by nuts to the casing. The mirror plates were glued to the control actuators with the help of pushers.

The back of the casing has a board on which three electric connectors are mounted. The protective casing and lid are made of Plexiglas and protect the control actuators and the optical surface of the mirror plate from accidental mechanical damage.

The model developed by us was investigated thoroughly. We shall present here only the main results of the tests. Table 1 shows the parameters of actuators at various stages of preparation of the mirror. Actuators 1, 3, 7 and 9 are located at the corners, 2, 4, 6 and 8 are located at the intermediate positions between the corners while actuator 5 is located at the centre.

The high average sensitivity of the actuators makes it possible to reduce the length of the active part of the actuator intended for the Iskra-6 facility by a factor of 2–4. The rigidity of the coupling between the casing and the mirror plate including the actuator and the attachment fittings was found to be 4–10 times lower than initial rigidity of the actuator itself. The tensile and compressive rigidities had a fourfold asymmetry for one actuator. The response functions were found to be different when positive and negative voltages were applied to the actuators (there was no symmetry), and response functions of actuators of the same type were also found to be different. The RMSD of response functions of the corner actuators (1, 3, 7, 9) was $0.3 \mu\text{m}$ for positive voltage and $-0.12 \mu\text{m}$ for negative voltage. In its turn, the RMSD of the response functions for intermediate actuators (2, 4, 6, 8) did not exceed $0.2 \mu\text{m}$ for positive voltage and $-0.13 \mu\text{m}$ for negative voltage. The RMSD of the response function for the central actuator was equal to $0.189 \mu\text{m}$ for both positive and negative voltages.

Hence, it can be concluded that in spite of further improvements in the construction and technology of preparation of mirrors, their parameters will be quite individual and strict certification of each mirror is required for a programme control of the compensation of ‘thermal’ aberrations.

However, the experimental and theoretical investigations indicate a satisfactory level of controllability of the mirrors. One can see from the interference patterns in Fig. 6 that it is

possible to attain a nearly perfect plane (the initial form had astigmatism with the number $N=4$ of bands on the interference pattern) and sphere. The surface shape was controlled by a computer through a special nine-channel control unit which ensured a voltage supply of ± 300 V to within 1 V at a frequency of up to 20 Hz.

The form of the ‘thermal’ aberration measured on the ‘Luch’ facility was ‘adjusted’ to the model mirror surface both theoretically (using the technique described in Sec. 4) and experimentally (using the measured response function of each actuator). The RMSD of theoretically obtained surface was $0.401 \mu\text{m}$ from the given value and $-0.467 \mu\text{m}$ from the experimental value (the experimentally determined

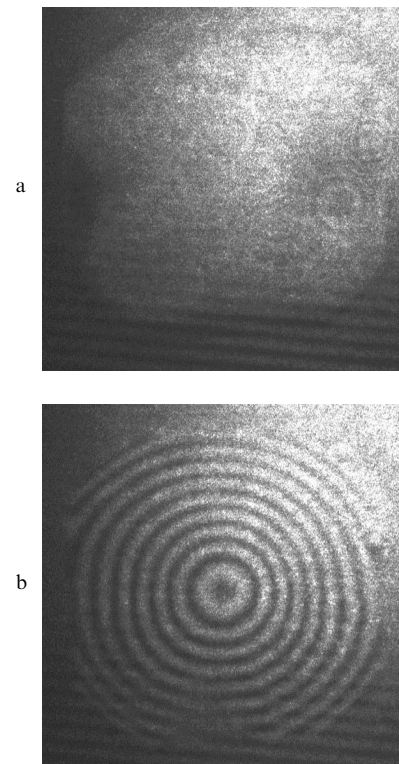


Figure 6. (a) Interference patterns of the initial shape of the surface after leveling and (b) after processing of the sphere.

error in the correction of such an aberration was found to be 0.6 μm in [7]).

6. Conclusions

The adaptive optical system devised for Iskra-6 is a phase conjugation system in which the deformable mirror is subjected to direct control from wavefront measurements as well as feedback control. It is expedient to install the WFS in such a system at the exit and the wide-aperture deformable mirror in the middle of the amplification path. The body of theoretical and experimental data was used to determine and substantiate the main parameters of the basic components of the optical system of the Iskra-6 facility – the wavefront sensor and the wide-aperture deformable mirror. A prototype of the WFS and a model of the DM have been designed, developed and tested.

References

1. LLNL. *ICF Quarterly Report. Special Issue: National Ignition Facility* (Virginia: Springfield, 1997) Vol. 7, No. 3.
2. Andre M.L. *Proc. SPIE Int. Soc. Opt. Eng.*, **3047**, 38 (1996).
3. Galakhov I.V., Garanin S.G., Eroshenko V.A., et al. *Fusion Engineering and Design*, **44**, 51 (1999).
4. Sukharev S.A., in. *Proc. III Intern. Conf. SSLA to ICF* (Monterey, Cal., 1998).
5. Voronich I.N., Galakhov I.V., Garanin S.G., et al. *Kvantovaya Elektron.*, **33**, 485 (2003) [*Quantum Electron.*, **33**, 485 (2003)].
6. Zacharias R.A., Beer N.R., Bliss E.S., et al. *Opt. Eng.*, **43** (12), 2873 (2004).
7. Voronich I.N., Garanin S.G., Zaretskii A.I., et al. *Kvantovaya Elektron.*, **35**, 140 (2005) [*Quantum Electron.*, **35**, 140 (2005)].
8. Tarasenko V.G., Shanin O.I. *Adaptivnaya optika v priborakh i ustroystvakh* (Adaptive Optics in Instruments and Devices) (Moscow: Federal Unitary Enterprise TsNIIATOMINFORM, 2005).
9. Alekseev V.N., Bessarab A.V., Garanin S.G., Dmitriev D.I., et al. *Opt. Zh.*, **9**, 11 (2002).
10. Fried D., in *Adaptivnaya optika* (Adaptive Optics) (Moscow: Mir, 1980).
11. Lyahov D.M., Shanin O.I. *Izv. Ross. Akad. Nauk., Ser. Fiz.*, **39**, 55 (1995).
12. Timoshenko S.P., Young D.H., Weaver W. *Kolebaniya v inzhenernom dele* (Vibrations in Engineering) (Moscow: Mashinostroenie, 1985).
13. Babayants G.I., Garanin S.G., Zhupanov V.G., et al. *Kvantovaya Elektron.*, **35**, 603 (2005) [*Quantum Electron.*, **35**, 603 (2005)].